# CORROSION RESISTANCE OF EXPERIMENTAL ALLOYS AND COATINGS UNDER SCW CONDITIONS

**Jian Li[1], W. Zheng[1], S. Kuyucak[1], J. Miles[2], W.Cook[2], O.T.Woo[3], Z. Zhou[4] and C. Ge[4]**

[1]CANMET - Materials Technology Laboratory, 183 Longwood Rd. S., Hamilton, ON, Canada
[2]University of New Brunswick, Fredericton, NB, Canada
[3] AECL Chalk River Laboratories, Chalk River, Ontario, Canada
[4]Beijing University of Science and Technology

## Abstract

Resistance to high temperature corrosion is one of the key challenges in future nuclear reactor material development. Iron-based materials with low Cr (<15%) content shows superior mechanical properties and high resistance to stress corrosion cracking. However, due to relatively low Cr and Ni contents, their corrosion resistances under SCW conditions are generally poor. High-Cr ferritic alloys, despite much improved corrosion resistance, are prone to embrittlement due to the precipitation of sigma phase in the microstructure. One of the materials solutions to overcome this will be to use structurally stable materials such as P91 or ODS steels as a substrate combined with a highly corrosion resistant surface coating. In this study, development of a metallic coating on P91 steel is discussed together with the evaluation of their SCW corrosion resistance. Microstructures of a few ODS steels are also evaluated.

**Keywords:** Corrosion, ODS, Coating

## 1. Introduction

Materials development has been a major focus in the international collaboration to develop Gen-IV nuclear reactors. The supercritical water-cooled reactor (SCWR) concept is one of the promising designs, in which water above its critical point (625$^{o}$C and 25 MPa) is the coolant in the reactor core. High-temperature mechanical properties, corrosion resistance and radiation damage are some of the key materials challenges. There has not been a single commercial material identified that meets all the requirements of the SCWR conditions.

There have been many reports on the SCW corrosion resistance of various types of commercial alloys. Studies by Allen [1] summarized SCW corrosion resistance of various alloys including Ni-based super alloys, stainless steels and ferritic/matensitic (F/M) steels. At temperatures between 500-600$^{o}$C, ferritic steels develop a thick but mechanically stable oxide layer, while austenitic alloys develop a thinner oxide layer. However, the thin oxide surface layer tends to spall off, resulting in weight loss. Ni-based alloys exhibited the lowest oxide thickness; however pitting was observed in the vicinity of intermetallic precipitates. Although Ni based alloys show good general corrosion resistance under SCW conditions [2-5], dissolution of major alloying components could pose significant problems [6]. For long term in-core applications, transmutation of Ni could also be a major concern. Even the corrosion resistant austenitic stainless steels (e.g. 316L) are susceptible to localized corrosion such as pitting, intergranular attack and stress corrosion cracking (SCC) [7].

Low Cr F/M steels exhibit excellent resistance to high-temperature creep and irradiation damage. Steels in this group are generally prone to corrosion under SCW conditions; however, it is suggested that corrosion resistance improves as Cr content increases [1]. The T/P91 class of high-temperature alloy has been widely used as piping and other components in fossil fuel plants at high-temperature locations. However with the relatively low chromium content (9%), it can not be used directly for in-core and out-of-core components in SCW reactors. An earlier study showed the formation of a thick oxide layer on T91 alloy surfaces after a SCW exposure of 500 hours at 500$^{o}$C [7]. Cr was found to be depleted in the outer oxide layer, while Mo was found to be concentrated in the inner layer.

Assessment of corrosion resistance needs data both from weight loss/gain measurements and detailed microscopy analysis. Some alloys with low weight loss/gains showed severely oxidized surfaces with a multi-layered oxide structure [1, 8]. Within the relatively short SCW exposure, the oxide films were stable and the oxide growth (or weight gain) appeared to follow a power law relationship. The long term stability of oxide films in reactor environments is largely unknown beyond about 5,000hr. Most of the previous studies on ferritic stainless steels used commercially available steels with relatively low Cr content. Our previous study showed superior corrosion resistance for a high-Cr steel (25% Cr) in SCW [10]. In this study, we have atomized this high-Cr steel and used its powder as a coating material on a commercial P91 alloy. SCW tests in a water loop showed much improved corrosion resistance over lower Cr alloys. In addition, microstructures data for Cr-steel oxide dispersion strengthened with $Y_2O_3$ are presented. SCW corrosion tests on these steels are reported in another paper in this symposium.

## 2. Experimental Details

A Fe-25%Cr steel was produced at CANMET-MTL to be processed as a coating material. This steel was air-melted and water-jet atomized. The chemical composition of the resulting steel powder is shown in Table 1. The average particle size (APS) of the powder was estimated to be 50 µm. The process produced a powder with a thin surface chromite layer, and the thickness is estimated to be 0.17 µm.

Small test coupons of 20 × 10 × 1 mm were machined from commercial P91 alloy and their surfaces were prepared using 600 grit SiC papers. A few test coupons were coated with the Fe-25%Cr powder using cold spray equipment. Both the coated and uncoated P91 coupons were sent to the University of New Brunswick and tested in their SCW loop (details of the system are presented elsewhere [10]). The autoclave temperature was 500ºC and SCW loop system pressure was steady at 25 MPa throughout the test duration of 500 hours. The neutral water had a conductivity of 0.5 – 0.7 µS/cm, and a low oxygen content of < 20 ppb measured continuously by an online electrochemical oxygen sensor inserted in the low temperature purification circuit in the test loop. Test coupons were taken out for weight change measurements at 100, 250 and 500 hours. After the test, the samples were sectioned and mounted in low shrinkage Epoxy resin. The cross-sections were polished and prepared for examination using an optical microscope and SEM.

Table -1 Chemical Composition of Fe-25%Cr steel (wt.%)

| C | Si | Mn | Cr | Mo | Cu | Ni | P | S | N | O |
|---|---|---|---|---|---|---|---|---|---|---|
| 0.026 | <0.01 | <0.05 | 24.5 | 0.30 | <0.01 | <0.01 | 0.003 | 0.003 | 0.028 | 0.430 |

## 3. Results

### 3.1 Powder Morphology

The atomized steel powder had a wide range of particle size distribution. A focused ion beam (FIB) microscope was used to reveal the microstructure of the powdered steel particles. The FIB technique has been used widely in both high-resolution imaging and site-specific TEM specimen preparation [11, 12]. Figure 1 shows FIB secondary electron image of the powder and an ion beam cross section of a typical particle. The particle shows a fully recrystallized structure with a thin layer of surface oxide (as indicated by the arrows in the micrograph). The microstructure of the powder particle could play an important role in the subsequent coating process. In general, the softer the powder particles are, the easier it is to apply them as coating material using the cold spray technique. The Fe-25%Cr is in general a hard material. However, with their relatively large and equiaxed grain structure, as shown in Figure 1, the powders should be relatively soft. Another concern is the presence of the surface oxide layer, which could prevent the powders from sticking to the substrate during cold spray.

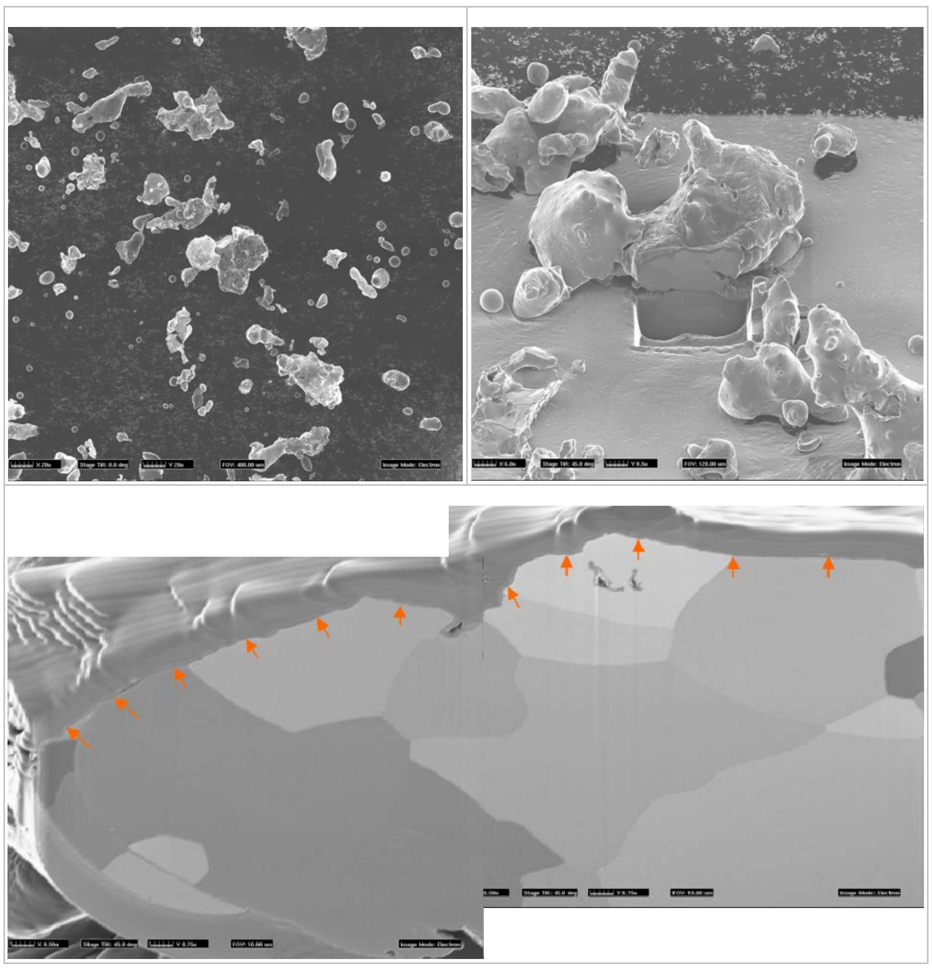

Figure 1 FIB secondary electron images showing the particle distribution and an ion beam cross sectioned view of a particle. The arrows point to the thin surface oxide layer.

### 3.2 Coating Microstructure

Cold spray of the Fe-25%Cr powder onto P91 substrate is not a straight forward process. The particles tend to bounce off the P91 alloy surface resulting in a rough surface similar to a sand blasting process. We had similar experience while attempting to coat a Zr-2.5%Nb pressure tube substrate using a relatively hard Ni powder. By optimizing our coating parameters, we were able to coat a very thin layer of Fe-25%Cr onto the P91 steel test coupons. A typical test coupon together with its cross sectional SEM image is shown in Figure 2. The coating on the surface appears to be very thin (~1-2 μm) and not quite continuous. Once the initial thin coating layer is established on the P91 surface, the incoming particles tend to bounce off the surface. We could not build up a thick coating using this method because of the following factors: hard substrate, relatively hard particles and the existence of an oxide layer on the particles.

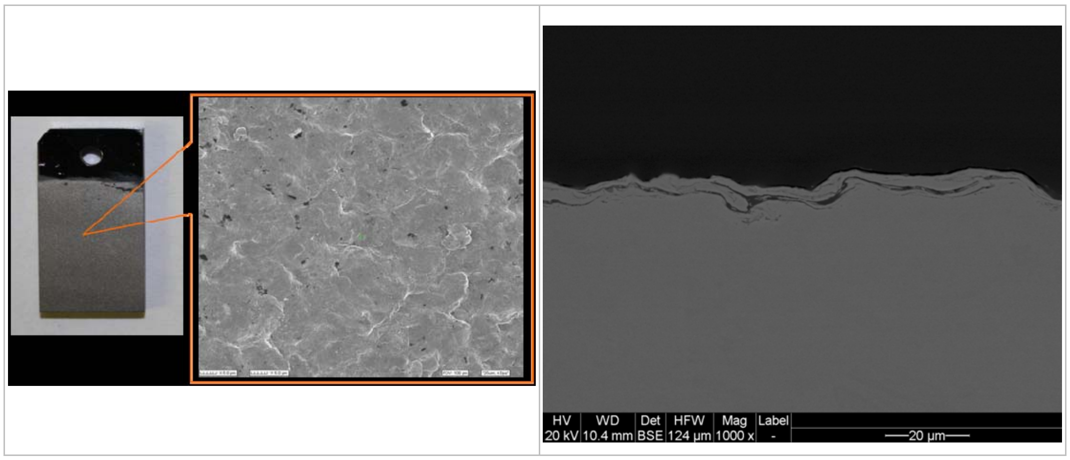


Figure 2 A cold sprayed test coupon and cross sectional view showing a thin and discontinuous coating layer

### 3.3 SCW Tests

During the 500 hour test, specimens were removed periodically from the autoclave for weight loss/gain measurements. As indicated in Figure 3, the uncoated P91 test coupons showed much higher weight gain compared to that of the coated steel coupons. Although the coating is very thin, it provided good corrosion protection to the P91 substrate during the course of the test.

The surfaces of the corroded samples were investigated using SEM. As shown in Figure 4a, the uncoated P91 surface is composed of a continuous iron-oxide (presumably magnetite) layer that forms as octahedral and tubular crystals, this is a commonly seen morphology on ferritic steels in SCW. The cross-sectional view of the sample in Figure 4b shows the typical multi-layered surface oxide. The top layer, indicated as location A, contains mostly iron oxide where Cr was not detected by EDS analysis. The inner layer is composed of an iron-chrome oxide beneath which there is evidence of internal oxidation between locations B and C. Figure 4c shows a typical area on the coated P91 surface after SCW exposure. Small patches of surface oxide have formed on the surface. Cross sectional view, as shown in Figure 4d indicated that these small oxide patches formed at locations where the coating was discontinuous and oxidation of the base P91 material is evident through the "mushroom-shaped" oxidation (location B) below the coating. Although the coating is thin and not quite continuous at this stage of our experiment, the oxide patches are quite small and only penetrated a very limited depth into the P91 substrate during the course of SCW exposure, and the coating continued to provide significant protection to the P91 substrate. The bulk Fe-25%Cr steel showed superior corrosion resistance under this SCW condition [13]. Further study, using thermal spray, is now under way to build up a thick and continuous coating on this P91 substrate.

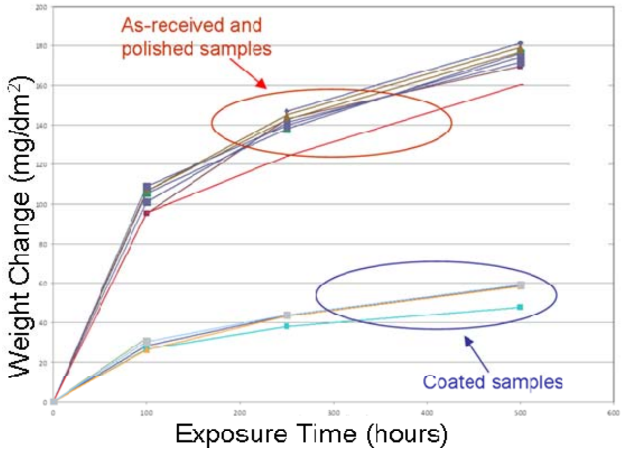


Figure 3 Weight-gain of uncoated and coated P91 test coupons after SCW exposure.

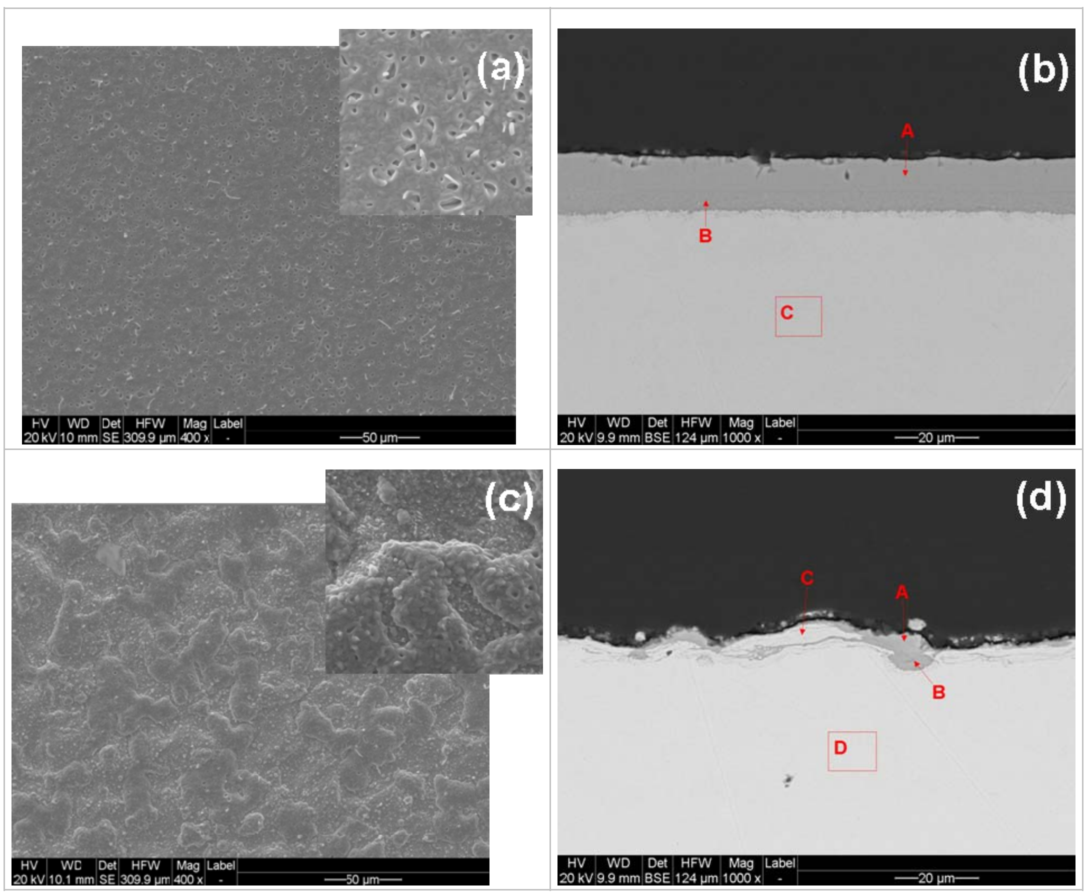


Figure 4 SEM images of test coupons after SCW exposure. (a) planview image of uncoated P91; (b) cross section of uncoated P91; (c) planview of coated P91; (d) cross section of coated P91

### 3.4 ODS Steel Morphology

Although difficult and expensive to process, ODS steels have been promising for high temperature applications due to their superior high temperature creep resistance.  A few experimental ODS steels were prepared at Beijing University of Science and Technology (Dr. Ge's group).  Microstructures of these steels were examined using a FIB microscope and a TEM. The size and distribution of $Y_2O_3$ nano particles in the steel matrix is of paramount importance in their high temperature performance. FIB images of the two typical ODS steels are shown in Figure 5.  Oxide particles are finely dispersed in the substrate in the low-Cr steel (martensitic). However, the higher Cr-steels (ferritic) appear to have large grains that are depleted of oxide nano-particles.  Although the high-Cr ODS steels have better corrosion resistance, they may not meet the strength requirement if a uniform distribution of dispersoids is not achieved.  On the other hand, the low-Cr martensitic ODS steels would need coatings to protect them from SCW corrosion.  The results of SCW corrosion tests of these ODS steels are reported in a separate paper in this symposium.

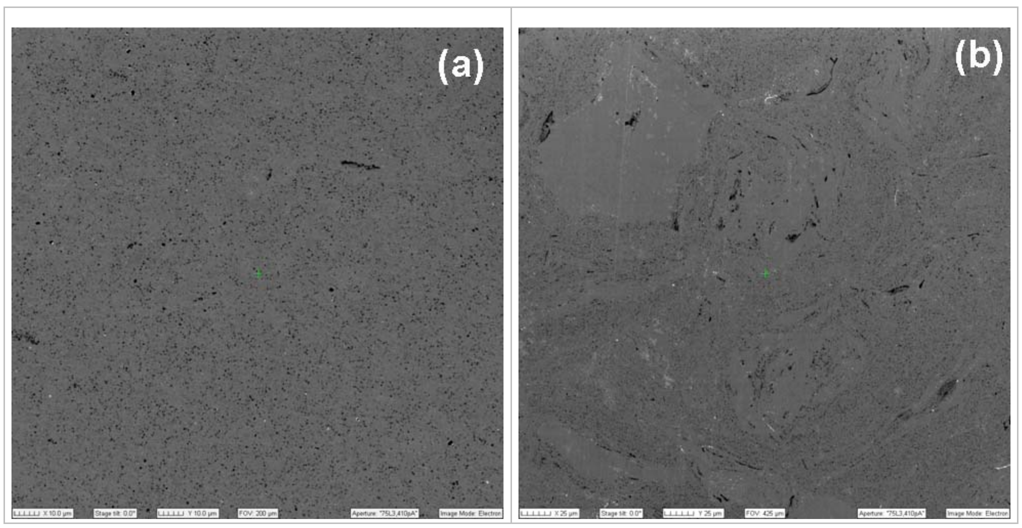


Figure 5 FIB secondary electron images of experimental ODS alloys, (a) 14%Cr ODS steel, and (b) 18%Cr ODS steel

Preliminary TEM work on the 18%Cr stainless steel was performed at AECL Chalk River Laboratory.  The bright-field TEM image shown in Figure 6a indicated a very fine grained microstructure.  However, the yttrium oxide particle is not quite visible using this imaging mode. EDS line scans in Figure 6b showed the yttrium oxide particles are associated with Ti.  Detailed TEM work will be published in a separate paper.

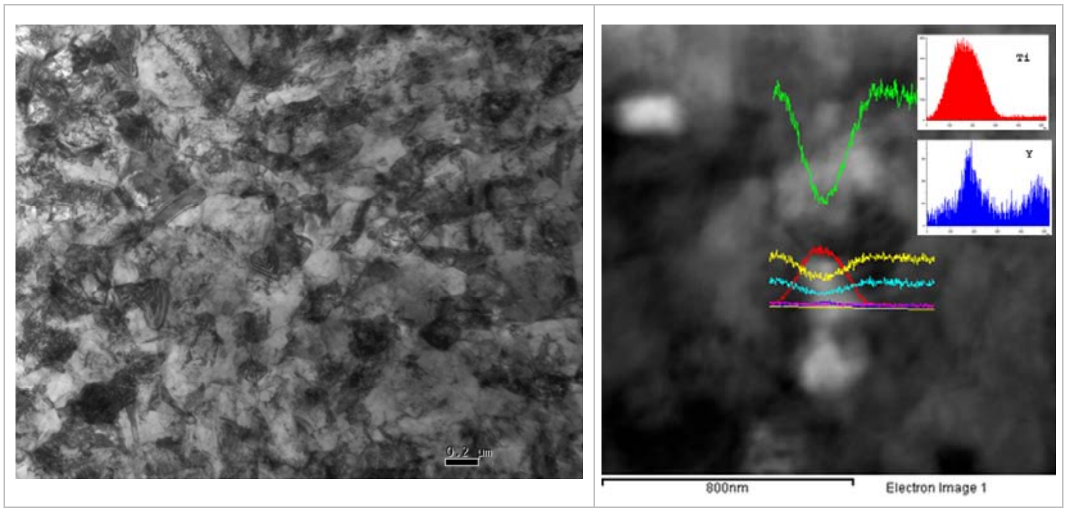


Figure 6 (a) Bright field TEM image, (b) STEM image and EDS line scans across Yttrium oxide particles

## 4. Summary

A high-Cr experimental steel (Fe-25%Cr) was prepared at the CANMET-MTL casting facility. This steel was used to produce a thin coating onto a commercial P91 steel substrate. SCW exposure at 500$^{o}$C, 25 MPa pressure for 500 hours indicated that this thin coating, although not continuous at this stage, reduced the SCW corrosion significantly. The limited corrosion observed is mainly due to the coating discontinuity. Work is underway to produce a thicker and continuous coating on P91 substrates using a thermal spray technique.

## 5. Acknowledgement

The authors would like to thank Mr. Mike Phaneuf, president of FIBICS Inc. for allowing us to access his FIB microscopes and the NSERC/NRCan/AECL Generation IV Technologies Program for funding.

## 6. References

[1] T.R. Allen, et al. 16th Pacific Basin Nuclear Conference, Aomori, Japan, Oct 13-18, 2008, Paper ID: P16P1032.
[2] G.T. Hong, et al. First Int. Workshop on Supercritical Water Oxidation, Jacksonville, Florida, Feb 6-9, 1995.
[3] P. Kritzer, et al. Corrosion 98, Paper No. 415, NACE, Houston, TX (1998).
[4] L.B. Kriksunov, et al., Journal of Electrochem. Soc., 4069, (1995).
[5] S. Huang, et al. ACS Symposium Series, 406, 287, ACS, Washington, DC (1998).
[6] Jian Li, et al. paper #56, 4th International Symposium on Supercritical Water-cooled Reactors, March 8-11, 2009, Heidelberg, Germany.
[7] D.B. Mitton, et al. Corrosion 2001, Paper No. 01352, NACE, Houston, TX, (2001).
[8] L. Tan, et al., Journal of Nuclear Materials, (2007), 371, 161-170.
[9] Y. Chen, et al. Corrosion Science, 48, 2843-2854, (2006).
[10] W. Cook, et al. 2nd Canada-China Workshop on Supercritical Water Reactors, Toronto, Canada, April 2010.

[11] Jian Li, chapter#4 in “New Material Science Research”, Nova Science Publishers Inc., Invited. Ed. Lawrence V. Olivante, Nova Science Publisher, ISBN-13: 978-1-60021-654-1, 2008.
[12] Jian Li, Journal of Metal, vol.58 No.3, 27-31, 2006.
[13] Yu Cheng Qian, et al. CANMET-MTL report MTL 2010-10(TR).